

## Theory of nonlinear cyclotron resonance in quasi-two-dimensional electron systems

S.Y. Liu and X.L. Lei

Department of Physics, Shanghai Jiaotong University, 1954 Huashan Rd., Shanghai 200030, China

Momentum and energy balance equations are developed for steady-state electron transport and optical absorption under the influence of a dc electric field, an intense ac electric field of terahertz (THz) frequency in a two-dimensional (2D) semiconductor in the presence of a strong magnetic field perpendicular to the 2D plane. These equations are applied to study the intensity-dependent cyclotron resonance (CR) in far-infrared transmission and THz-radiation-induced photoconductivity of GaAs heterostructures in Faraday geometry. We find that the CR peaks and line shapes of the transmittance exhibit different intensity dependence when the intensity of THz field increases in the range above or below a certain critical value. The CR in photoresistivity, however, always enhances with increasing the intensity of the THz field. These results qualitatively agree with the experimental observations. We have clarified that the CR in photoconductivity is not only the result of the electron heating, but also comes from photon-assisted scattering enhancement, especially at high temperatures. The effects of an intense THz field on Faraday angle and ellipticity of magnetically-biased 2D semiconductors have also been demonstrated.

PACS numbers: 73.50.Jt, 73.50.Mx, 78.67.De, 78.20.Ls

## I. INTRODUCTION

Cyclotron resonance (CR) is a fundamental process of carriers in quasi-two-dimensional semiconductors subjected simultaneously to a magnetic field and a far-infrared or terahertz (THz) ac field. It occurs when the separation between two adjacent Landau levels is closed to the photon energy of the ac field, and leads to the resonant behavior in absorption and in photoconductivity as functions of the magnetic field.

CR in absorption or transmission has been proved to be a powerful tool providing valuable information of two-dimensional (2D) semiconductors on the carrier scattering processes, the conning potential, and even the spin relaxation mechanisms.<sup>1</sup> Generally, weak far-infrared irradiations were used in most of experiments, and theoretical analyses focused on the linear response of the system to the ac field.<sup>2</sup> When the strength of the incident radiation field increased, nonlinear behavior of CR in absorption and transmission was observed. It was found<sup>3</sup> that the resonant field to zero field transmissivity ratio descended slightly with increasing the intensity of the far-infrared field from  $0.1 \text{ W/cm}^2$ , then increased for radiation-field intensities above  $10 \text{ W/cm}^2$ . This kind of intensity-dependent CR transmission has not yet been explained so far except a simple comparison with linear-response formula of Drude-type taking the scattering time as a fitting parameter.

Another manifestation of CR shows up in photoresponse, namely, photoconductivity or photoresistivity. The latter is defined as the longitudinal dc magnetoresistivity change induced by the irradiation of the high-frequency electromagnetic wave, which exhibits a resonant peak structure under CR condition. This effect has long been known at low temperatures, and was believed to arise from the electron heating induced redistribution of the electron gas upon absorbing the radiation-field energy.<sup>4,5</sup> The energy absorption and thus the rise of the electron temperature exhibit maxima when the photon energy of the radiation field equals the cyclotron energy, yielding the resonance peak structure of the photoresistivity. Later analysis of experimental data<sup>6</sup> indicated that, in addition to this heating-induced electron redistribution, another nonthermal mechanism might be needed to account for the observed photoconductivity of GaAs/AlGaAs heterostructures at CR. Recent photoresistivity measurement of GaAs/AlGaAs heterojunction performing at lattice temperature  $T = 150 \text{ K}$  subjected to irradiations of 4 THz frequency,<sup>7</sup> surprisingly showed remarkable CR peaks. At such a high lattice temperature with strong polar optic phonon scattering providing an efficient energy dissipation channel, the radiation-induced electron-temperature increase is far smaller to account for such strong CR in photoresistivity. So far no convincing nonthermal mechanism responsible for far-infrared photoconductivity in semiconductors has been proposed. A nonlinear theory for high-temperature photoresistivity CR in two-dimensional system is still lacking. It is an urgent need to develop a tractable, microscopic theory capable of treating nonlinear absorption and photoresponse under intense THz radiation and to clarify the missing nonthermal mechanism for high-temperature photoresistivity in two-dimensional semiconductors.

A few years ago, one of the authors developed a balance-equation approach<sup>8</sup> for hot-electron transport driven by a THz electric field of single frequency ( $E_1 \sin(\omega t)$ ). This method made use of the fact that, when the harmonic generation is small and the frequency gets into the THz regime or higher, the electron drift velocity in the steady transport state oscillates almost out of phase of the electric field, i.e. the drift velocity is essentially of the form  $v_1 \cos(\omega t)$ . At the same time, all orders of this (frequency!) photon assisted in-purity and phonon scatterings are included in the relaxation processes. This method has been successfully applied to discuss THz photoabsorption and

THz-induced dc conductivity response in bulk and two-dimensional semiconductors in the case without magnetic field<sup>8,9</sup> or with a magnetic field in Voigt configuration.<sup>10</sup> However, this assumption of such time-dependent form of drift velocity will no longer be true when there is a strong magnetic field  $B$  not parallel to  $v_1$ . Since the Lorentz force  $e\mathbf{v}_1 \times \mathbf{B} \cos(\omega t)$  acts on the moving electron, its steady-state drift velocity will contain a term  $(\omega_c = \omega) v_1 \sin(\omega t)$ , where  $\omega_c = \frac{eB}{m}$  is the cyclotron frequency. This velocity, which is perpendicular to  $v_1$  and  $B$ , and oscillates  $\pi/2$  out of phase of  $v_1 \cos(\omega t)$ , is of the same order of magnitude as  $v_1$  in the frequency and magnetic field range  $\omega \sim \omega_c$ . Because of this, the balance-equation method used in Ref.10 is not able to deal with the problem related to cyclotron resonance in semiconductors in Faraday geometry.

The purpose of this article is to develop a theory for electron transport driven by an intense far-infrared electric field in a quasi-2D semiconductor in the presence of an arbitrary magnetic field perpendicular to the 2D plane. We find that it is possible to extend balance equation method proposed in Ref.8 to the case in the presence of a quantized magnetic field in Faraday configuration, and to deal with those problems in magnetotransport, such as the intensity-dependent THz transmission and photoresponse at CR in quasi-2D electron systems.

This paper is organized as follows. In Sec.II we will sketch the derivation of the force- and energy-balance equations of quasi-two-dimensional electron systems subjected to a magnetic field, an arbitrary dc and THz ac electric fields. In Sec.III the cyclotron resonance in time-dependent drift velocity is discussed. The investigation on cyclotron resonance in transmission and photoconductivity is, respectively, presented in Sec.IV and Sec.V. Finally, in Section VI a short conclusion will be given.

## II. FORMULATION

### A. Hamiltonian

We consider  $N_e$  electrons in a unit area of a quasi-two-dimensional system, such as a heterojunction or a quantum well. In these systems the electrons are free to move in the x-y plane, but are subjected to a confining potential  $V(z)$  in the z-direction. These electrons are interacting with each other and also coupled with phonons and scattered by randomly distributed impurities in the lattice.

To include possible elliptically polarized electromagnetic radiation we assume that a uniform dc electric field  $E_0$  and a terahertz ac field  $E(t)$  of angular frequency  $\omega$ ,

$$E(t) = E_s \sin(\omega t) + E_c \cos(\omega t); \quad (1)$$

are applied in the x-y plane, together with a uniform magnetic field  $\mathbf{B} = (0; 0; B)$  along the z axis. These magnetic and electric fields can respectively be described by a vector potential  $\mathbf{A}(r)$  and a scalar potential  $\phi(r; t)$  of the form

$$\mathbf{r} \times \mathbf{A}(r) = B \hat{z}; \quad (2)$$

$$\phi(r; t) = -\mathbf{r} \cdot \mathbf{E}(t); \quad (3)$$

In the presence of these electric and magnetic fields the Hamiltonian of the system has the form

$$H = H_{eE}(t) + H_{ei} + H_{ep} + H_{ph}; \quad (4)$$

Here

$$H_{eE}(t) = \sum_j \left[ \frac{1}{2m} p_{jk}^2 - eA(r_{jk})^2 + \phi(r_{jk}; t) + \frac{p_{jz}^2}{2m_z} + V(z_j) \right] + \sum_{i < j} V_c(r_{ik} - r_{jk}; z_i; z_j) \quad (5)$$

is the Hamiltonian of electrons driven by the electric and magnetic fields with  $V_c$  being the electron-electron Coulomb interaction,  $H_{ei}$  and  $H_{ep}$  are, respectively, the electron-impurity and electron-phonon couplings. In equation (5),  $r_{jk} = (x_j; y_j)$  and  $p_{jk} = (p_{jx}; p_{jy})$  are the coordinate and momentum of the  $j$ th electron in the 2D plane, and  $z$  and  $p_{jz}$  are those perpendicular to the plane;  $m$  and  $m_z$  are, respectively, the effective mass parallel and perpendicular to the plane.

It is convenient to introduce two-dimensional center-of-mass momentum and coordinate variables  $\mathbf{P} = (P_x; P_y)$  and  $\mathbf{R} = (R_x; R_y)$ :

$$\mathbf{P} = \sum_j \mathbf{p}_{jk}; \quad \mathbf{R} = \frac{1}{N_e} \sum_j \mathbf{r}_{jk} \quad (6)$$

and the relative-electron momentum and coordinate variables  $p_j^0 = (p_{jk}^0; p_{jz})$  and  $r^0 = (r_{jk}^0; z_j)$  ( $j = 1; \dots; N_e$ ):

$$p_{jk}^0 = p_{jk} - \frac{1}{N_e} P; \quad r_{jk}^0 = r_{jk} - R; \quad (7)$$

In term of these variables, the Hamiltonian  $H_{eE}$  can be separated into a center-of-mass part  $H_{cm}$  and a relative electron part  $H_{er}$ :

$$H_{eE} = H_{cm} + H_{er}; \quad (8)$$

$$H_{cm} = \frac{1}{2N_e m} (P - N_e e A(R))^2 - N_e e E_0 R - N_e e E(t) R; \quad (9)$$

$$H_{er} = \sum_j \left[ \frac{1}{2m} p_{jk}^0{}^2 - e A(r_{jk}^0)^2 + \frac{p_{jz}^2}{2m_z} + V(z_j) + \sum_{i < j} V_c(r_{ik}^0, r_{jk}^0; z_i, z_j) \right]; \quad (10)$$

It should be noted that the relative-electron Hamiltonian  $H_{er}$  is the just that of a quasi-2D system subjected to a uniform magnetic field in the  $z$  direction. Its eigenstate can be designated by a subband index  $s$ , a Landau level index  $n$  and a wavevector  $k_y$ , having energy spectrum

$$\epsilon_{sn} = \epsilon_s + (n + \frac{1}{2}) \hbar \omega_c; \quad s = 0, 1, \dots; \quad \text{and} \quad n = 1, 2, \dots; \quad (11)$$

where  $\omega_c = \hbar B / m$  is the cyclotron frequency. In this paper we will limit to the case that the 2D electrons occupying only the lowest subband and ignore index  $s$ . In Eq. (5) the electron-impurity and electron-phonon interaction  $H_{ei}$  and  $H_{ep}$  have the same expression as those given in Ref.11, in terms of center-of-mass coordinate  $R$  and the density operator of the relative-electrons,

$$\rho_k = \sum_j e^{i q_k \cdot r_j^0}; \quad (12)$$

## B. Balance equations

On the basis of the Heisenberg equation of motion we can derive the velocity (operator) of the center-of-mass,  $V$ , which is the rate of change of the center-of-mass coordinate  $R$ , and equation for the rate of change of the center-of-mass velocity  $V - \dot{R}$ :

$$V = i[R; H] = \frac{1}{N_e m} (P - N_e e A(R)); \quad (13)$$

and

$$\dot{V} = i[V; H] + \frac{\partial V}{\partial t} = \frac{e}{m} \hbar E_0 + E(t) + V \times B + \frac{F}{N_e m}; \quad (14)$$

with

$$F = i \sum_{q_k, z_a} U(q_k; z_a) \rho_k e^{i q_k \cdot (R - r_a)} - i \sum_{q; } M(q; ) \rho_q e^{i q_k \cdot R} \rho_{-q_k}; \quad (15)$$

We can also derive equation for the rate of change of the relative electron energy:

$$\dot{H}_{er} = i[H_{er}; H] = i \sum_{q_k, z_a} U(q_k; z_a) e^{i q_k \cdot (R - r_a)} \rho_{-q_k} - i \sum_{q; } M(q; ) \rho_q e^{i q_k \cdot R} \rho_{-q_k}; \quad (16)$$

In Eqs. (15,16)  $(r_a, z_a)$  and  $U(q_k; z_a)$  are the impurity position and its potential,  $M(q; )$  is the matrix element due to coupling between electrons and a phonon of wave vector  $q = (q_k, q_z)$  in branch having energy  $\epsilon_q$ ,  $\epsilon_q = \hbar \omega_q + \hbar^2 q_z^2 / 2m_z$  stands for the phonon field operator, and  $\rho_{-q_k} = i[q_k; H_{er}]$ .

In order to derive the force- and energy-balance equations we need to carry out the statistical average of these operator equations. As proposed in Ref.12, we treat the center-of-mass coordinate  $R$  and velocity  $V$  classically, and by neglecting their small fluctuations we will regard them as time-dependent expectation values of the center-of-mass



In these expressions,  $q_k = \sqrt{k^2 + \epsilon_0 U(q_k)}$  is related to the impurity potential  $U(q_k; z_a)$  and distribution of impurities along  $z$  axis  $n_i(z)$ ;  $\chi_2(q; \omega)$  is the imaginary part of the electron-phonon correlation function, which can be expressed through the imaginary part of electron density correlation function  $\chi_2(q_k; \omega)$  as<sup>15</sup>

$$\chi_2(q; \omega) = 2 \chi_2(q_k; \omega) n \frac{q}{T} = n \frac{q}{T_e}; \quad (24)$$

with  $n(x) = 1/[\exp(x) + 1]$  being the Bose function. The real parts of the electron-phonon correlation function and the electron density correlation function,  $\chi_1(q; \omega)$  and  $\chi_1(q_k; \omega)$ , can be obtained from their imaginary parts through Kramers-Kronig transformation.<sup>15</sup>

The momentum balance equation obtained by taking the statistical average of operator equation (14), has the following form

$$v_1 \sin(\omega t) - v_2 \cos(\omega t) = \frac{1}{N_e m} F(t) + \frac{e}{m} \hbar E_0 + E(t) + [v_0 + v(t)] \hbar g; \quad (25)$$

That is

$$0 = N_e e E_0 + N_e e (v_0 - \hbar g) + F_0; \quad (26)$$

$$v_1 = \frac{e E_s}{m \omega} - \frac{1}{N_e m \omega} (F_{11} - F_{22}) - \frac{e}{m \omega} (v_2 - \hbar g); \quad (27)$$

$$v_2 = \frac{e E_c}{m \omega} + \frac{1}{N_e m \omega} (F_{12} + F_{21}) - \frac{e}{m \omega} (v_1 - \hbar g); \quad (28)$$

The energy-balance equation is obtained by taking the long-time average of statistically averaged operator equation (16) to be

$$N_e e E_0 - \hbar g + S_p - W = 0; \quad (29)$$

Here  $W$  is the time-averaged rate of the energy transfer from the electron system to the phonon system, whose expression can be obtained from the second term on the right side of equation (21) by replacing the  $q_k$  factor with  $q$ .  $S_p$  is the time-averaged rate of the electron energy gain from the radiation field and has the following form

$$S_p = \sum_{q_k} U(q_k)^2 \sum_{n=1}^{\infty} n! J_n^2(\omega) \chi_2(q_k; \omega) + \sum_{q; \omega} \hbar g(q; \omega)^2 \sum_{n=1}^{\infty} n! J_n^2(\omega) \chi_2(q; \omega) + q \chi_2(q; \omega); \quad (30)$$

Note that  $S_p$  is negatively equal to time averaged Joule heat  $\langle \dot{Q} \rangle = N_e e (E_0 - \hbar g + E_s - \hbar g + E_c - \hbar g)$ .

Momentum and energy balance equations (26) to (29) constitute a close set of equations to determine the parameters  $v_0, v_1, v_2$ , and  $T_e$  when  $E_0, E_c$  and  $E_s$  are given.

The sum over  $n$  in the expressions for  $F_0, F$ ,  $W$  and  $S_p$  represents contribution of all orders of multiphoton processes related to the photons of frequency  $\omega$ . In the present formulation, the role of the single-frequency radiation field is two fold. (1) It induces photon-assisted impurity and phonon scatterings associated with single ( $j=1$ ) and multiple ( $j>1$ ) photon processes, which are superposed on the direct impurity and phonon scattering ( $n=0$ ) term. (2) It transfers energy to the electron system ( $S_p$ ) through single and multiple photon-assisted process.

Note that  $\chi_2(q_k; \omega)$  and  $\chi_1(q_k; \omega)$  are respectively the imaginary and real parts of the electron density correlation function of the 2D system in the presence of the magnetic field. In the Landau representation, one can write<sup>2</sup>

$$\chi_2(q_k; \omega) = \frac{1}{2} \frac{X}{l^2} \sum_{n,m=0}^{\infty} C_{n,m} (l^2 q_k^2 = 2) \chi_2(n; n^0; \omega); \quad (31)$$

$$\chi_2(n; n^0; \omega) = \frac{2}{\omega} \text{d}'' [f(\omega) - f(\omega + \omega_n)] \text{Im} G_n^r(\omega + \omega_n) \text{Im} G_{n^0}^r(\omega); \quad (32)$$

where  $l = \sqrt{\hbar / 2eB}$  is the magnetic length,

$$C_{n,n+1}(Y) = \frac{n!}{(n+1)!} Y^{1/2} e^{-Y} [L_n^1(Y)]^2 \quad (33)$$

with  $L_n^1(Y)$  being the associate Laguerre polynomial,  $f(\epsilon) = \exp[(\epsilon - T_e)/k_B T_e]$  is the Fermi distribution function, and  $\text{Im} G_n^r(\epsilon)$  is the imaginary part of the Green's function of the Landau level  $n$ , which is proportional to the density of states, such that the density of electrons is given by

$$N_e = \sum_n \int_{-\infty}^{\infty} d\epsilon f(\epsilon) \text{Im} G_n^r(\epsilon); \quad (34)$$

This equation determines the chemical potential.

In principle, to obtain the Green's function of Landau levels  $n$ ,  $G_n^r(\epsilon)$ , a self-consistent calculation has to be carried out from the Dyson equation for the selfenergy with all the scattering mechanisms included.<sup>16</sup> The resultant Green's function is generally a complicated function of the magnetic field, temperature, and Landau-level index  $n$ , also dependent on the relative strength of the impurity and phonon scattering. In the present study we do not attempt a self-consistent calculation of  $G_n^r(\epsilon)$ . Instead, we choose a Gaussian-type function for the Landau-level shape for simplicity,<sup>17</sup>

$$G_n^r(\epsilon) = i(\epsilon) \exp[-i(n + \frac{1}{2})\epsilon t - \frac{1}{2} \epsilon_n^2 t^2] \quad (35)$$

with a unified broadening parameter  $\epsilon_n = \epsilon_0$  for all the Landau levels, which is taken as  $(2e\hbar^2/m_0)^{1/2}$ . When the hot-electron effect is neglected,  $\epsilon_0$  corresponds to the linear mobility at temperature  $T$  in the absence of magnetic fields.<sup>18</sup> In order to consider the hot-electron-induced Landau levels broadening, we will empirically treat  $\epsilon_0$  as the linear mobility of the system in the absence of the magnetic field at temperature  $T_e$ . Note that this Gaussian-type of Green's function is proved to be correct at low temperature.<sup>19</sup> On the other hand, it also has been used to interpret the magnetophonon resonance at high lattice temperature.<sup>20</sup> In the present paper we will show that this Green's function can lead to a qualitative agreement between theoretical and experimental results within the magnetic field range considered. To improve the agreement further, a more careful study on the Green's function of a Landau level should be performed.<sup>16</sup>

Above formulation can be used to describe the transport and optical properties of magnetically-biased quasi-2D semiconductors subjected to a dc field and a terahertz field. The conventional magneto-optical study in the far-infrared frequency regime corresponds to the case of zero dc field  $E_0 = 0$ , where one studies the intensity-dependent terahertz absorption, transmission and other effects in the presence of a strong magnetic field. On the other hand, to investigate photoconductivity, we should treat the weak dc field limit of our formulation.

### III. CYCLOTRON RESONANCE IN DRIFT VELOCITY

Substituting the force Eq. (27) into Eq. (28), we can write

$$v_1 = (1 - \epsilon_c^2)^{-1} \frac{e\hbar}{m!} E_s + \frac{e}{m!} (E_c - B) \frac{i}{N_e m!} [F_{11} - F_{22}] + \frac{e}{m!} [(F_{12} + F_{21}) - B]; \quad (36)$$

$$v_2 = (1 - \epsilon_c^2)^{-1} \frac{e\hbar}{m!} E_c - \frac{e}{m!} (E_s - B) + \frac{1}{N_e m!} [F_{12} + F_{21}] + \frac{e}{m!} [(F_{11} - F_{22}) - B]; \quad (37)$$

Cyclotron resonance is easily seen in the case of weak scatterings when the terms with  $F$  functions in the above equation are small: both  $v_1$  and  $v_2$  exhibit peaks at CR. Since all the transport quantities, including  $W$ ,  $S_p$  and  $F_0$ , are functions of the drift velocity as well as the electron temperature  $T_e$ , and the latter is determined by the energy balance equation (30), the CR of  $v_1$  and  $v_2$  will result in the CR in  $W$ ,  $S_p$ ,  $F_0$  and  $T_e$ .

Eqs. (36) and (37) can be further simplified when the radiation field is weak and the dc field is absent. In this case  $v$  can be treated as small parameters. To the first order of these small parameters, the force function  $F$  can be written as

$$F = N_e m v M(\epsilon; v_0) \quad (\epsilon = 1; 2); \quad (38)$$

where  $M(\epsilon; v_0)$  are the real ( $\epsilon = 1$ ) and imaginary ( $\epsilon = 2$ ) parts of the memory functions.<sup>15</sup> It is convenient to write out the expression for the complex velocity  $v_+ = v_{1x} + iv_{2x}$  and  $v_- = v_{2y} - iv_{1y}$  rather than for  $v_1$  and  $v_2$

$$\begin{aligned} v_+ &= e\hbar/2m \frac{E_+}{(\epsilon - \epsilon_c) + i} + \frac{E_-}{(\epsilon + \epsilon_c) + i}; \\ v_- &= e\hbar/2m \frac{E_+}{(\epsilon - \epsilon_c) + i} - \frac{E_-}{(\epsilon + \epsilon_c) + i}; \end{aligned} \quad (39)$$

Here, we have defined

$$\begin{aligned} m &= m [1 + M_1(!; v_0) = !]; \\ 1 &= M_2(!; v_0) = [1 + M_1(!; v_0) = !]; \\ !_c &= eB/m; \\ E_+ &= E_{sx} + E_{cy} + i(E_{sy} - E_{cx}); \\ E_- &= E_{sx} - E_{cy} - i(E_{sy} + E_{cx}); \end{aligned}$$

with  $(E_{sx}; E_{sy}) = E_s$  and  $(E_{cx}; E_{cy}) = E_c$ .

Our weak-field results for  $v_1$  and  $v_2$  reduces to those of Ref.2 in the case of circularly polarized ac elds.

#### IV . TRANSMISSION

For normally incident electromagnetic wave, the transmitted electric eld  $E(t)$ , which is regarded as the eld driving the 2D electrons,<sup>21</sup> is related to the incident electric eld  $E_i(t)$  by

$$E(t) = \frac{N_e e v(t) =_0 c}{n_s + n_0} + \frac{2n_0}{n_s + n_0} E_i(t); \quad (40)$$

Here  $n_0$  and  $n_s$  are the relative refractive indices of the air and 2D semiconductor, and  $c$  and  $_0$  are the light speed and the dielectric constant in vacuum, respectively. The transmitted eld  $E(t)$  depends on the drift velocity  $v(t)$  of the 2D system. In the following numerical studies on transmission and photoconductivity, we will assume a sinusoidal incident eld  $E_i(t) = (E_{is} \sin(!t); 0)$  along  $x$  axis and derive  $E(t)$  self-consistently together with  $v(t)$ .

We have numerically calculated the magneto-optical properties of a GaAs/AlGaAs heterojunction subjected to a THz ac eld and a magnetic eld. The strength of transmitted ac eld  $E(t)$ , and the parameters  $v$  ( $= 1, 2$ ) and  $T_e$ , are obtained by resolving the Eqs.(40), (27), (28) and (29). We consider a GaAs-based quasi-2D system having electron density  $N_e = 2.5 \times 10^{15} \text{ m}^{-2}$  and 4.2K linear mobility  $50 \text{ m}^2/\text{Vs}$  (which is used to determine the impurity density) at lattice temperature  $T = 4.2 \text{ K}$ , similar to that used in Ref.3. The elastic scattering due to randomly distributed charged impurity and the inelastic scattering due to polar optical phonons (via Frohlich coupling with electrons), longitudinal acoustic phonons (via deformation potential and piezoelectric coupling), and transverse acoustic phonons (via piezoelectric coupling with electrons) are taken into account. The material and electron-phonon coupling parameters are taken as typical values for GaAs. In the numerical calculation the maximum Landau level is taken to be 20, and the summation over multiphoton indices  $n$  are carried up to a given accuracy of  $10^{-3}$  for each quantity.

The transmittance  $T$ , defined as<sup>21</sup>

$$T = \frac{\langle E(t)^2 \rangle_t}{\langle E_i(t)^2 \rangle_t} \quad (41)$$

with  $\langle \cdot \rangle_t$  denoting the time average. When connecting it with measured quantities, of course, the multiple interference between interfaces of the substrate has to be taken into account. The calculated transmittance and the corresponding electron temperature are plotted in Fig.1 as functions of the intensity of the THz eld at two frequencies  $! = 0.83$  and  $1.6 \text{ THz}$  in the center position of CR, namely  $!_c = !$ . It can be seen that, the transmittance first decreases gently with increasing intensity of the THz radiation from zero, and reaches a bottom at a critical intensity around  $10 \text{ W/cm}^2$ , then increases rapidly with further increasing the eld strength. This feature appears more pronounced at lower frequency, in consistence with the experimental observation,<sup>3</sup> as shown in the inset of Fig.1, where the measured transmittance for  $1.6 \text{ THz}$  and  $0.24 \text{ THz}$  exhibits similar trend. The case of  $0.83 \text{ THz}$  does not show minimum. This deviation is believed to come from the experimental errors. In Fig.2 we display the transmittance CR line shape for incident electromagnetic elds of different intensities at frequency  $0.83 \text{ THz}$ . The line width exhibits no significant change below the critical intensity but increases rapidly when the intensity of THz eld grows above the critical value.

This kind of  $E_{is}$ -dependent behavior of transmittance is in agreement with the intensity dependence of the absorption rate  $S_p = E_{is}^2$  in the absence of the magnetic eld. For a similar 2D GaAs-based semiconductor without magnetic eld, Ref.9 showed that, the absorption percentage increases with increasing strength of the radiation eld from low-field value, then reaches a maximum (of order of 2 percent) at the eld amplitude around several  $\text{kV/cm}$  before decreasing with further increase of the radiation eld strength, and that lower frequency has stronger maximum. At low velocity side, when hot-electron effect is relatively weak and the direct impurity and phonon scatterings

change little, the behavior of the absorption rate comes mainly from the drift-velocity dependence of the multiphoton assisted scattering matrix element, as described by the Bessel functions  $J_n^2(\cdot)$  in the expressions for  $S_p$ . In fact, all the multiphoton ( $n \geq 1$ ) contributions to the absorption coefficient are zero at vanishing velocity and reach maximum at finite (increasing with  $n$ ) drift velocities, the resultant absorption coefficient first increases with increasing velocity. When the drift velocity becomes sufficiently large, reduction of absorption rates, induced by the large argument of the lowest-order Bessel functions, will exceed the increased contributions from the other multiphoton processes. This leads to the drop of the absorption rate. In the present case having a strong magnetic field, CR greatly enhances the drift velocity  $v_1$  and  $v_2$  at  $\omega_c = \omega$  for a given  $E_{is}$  in comparison with the case without magnetic field. Therefore, the maximum absorption rate should appear at much smaller strength of radiation field and have much larger value for the case of cyclotron resonance than in the absence of a magnetic field or far away from CR.

The behavior of the transmittance CR line shape is related to Landau level broadening due to hot-electron effect. For THz field below the critical intensity the electron temperature is less than 60 K (see Fig.1) and impurities are the dominant scatterers, yielding almost a constant mobility  $\mu_0$  (thus the Landau level broadening). When the THz field goes above the critical intensity, the electron temperature grows rapidly and polar optical phonons become the dominant scatterers, giving rise to a strongly temperature-dependent mobility  $\mu_0$ , thus a Landau level broadening which increases rapidly with increasing field strength.

Our formulation can also be employed to investigate the change of the transmitted electromagnetic field polarization in quasi-two-dimensional electron systems. This effect is known as Faraday effect and has long been investigated under linear condition.<sup>22,23,24</sup> The present approach provides a convenient formulation to study the Faraday effect for the case when the incident light is strong and the nonlinear absorption occurs.

The relevant quantities characterizing the Faraday effects are the ellipticity  $\epsilon$  and Faraday rotation angle  $\theta_F$ , which are determined through the amplitudes of transmitted field  $E(t)$

$$\tan \epsilon = (a^+ - a) / (a^+ + a); \quad (42)$$

$$\theta_F = (\phi^+ - \phi) / 2; \quad (43)$$

Where

$$\tan \epsilon^+ = \frac{E_{sx} + E_{cy}}{E_{cx} - E_{sy}}; \quad (44)$$

$$\tan \epsilon^- = \frac{E_{sx} - E_{cy}}{E_{cx} + E_{sy}}; \quad (45)$$

$$a^+ = \frac{q}{(E_{sx} + E_{cy})^2 + (E_{cx} - E_{sy})^2}; \quad (46)$$

$$a^- = \frac{q}{(E_{sx} - E_{cy})^2 + (E_{cx} + E_{sy})^2}; \quad (47)$$

with  $(E_{sx}; E_{sy}) = E_s$  and  $(E_{cx}; E_{cy}) = E_c$ .

We plot the calculated results of  $\epsilon$  and  $\theta_F$  in Fig.3 for the above mentioned two-dimensional sample. The resonance in ellipticity and antiresonance in Faraday angle can be seen evidently. Their line shapes also manifest different behavior when the intensity of THz field lies below or above the critical value. These intensity-dependent behaviors of ellipticity and Faraday rotation can also be understood by multiphoton-assisted scatterings and hot-electron effect induced Landau level broadening.

## V. PHOTOCONDUCTIVITY

The response of the linear dc conductance to far-infrared irradiation is easily obtained in the weak dc field limit of our formulation. Taking  $v_0$  to be in the x direction,  $v_0 = (v_{0x}; 0; 0)$  and expanding the equation (26) to the first order in  $v_{0x}$ , we obtain the transverse and longitudinal resistivities  $R_{xy}$  and  $R_{xx}$  as follows:

$$R_{xy} = \frac{E_{0y}}{N_e e v_{0x}} = B = N_e e; \quad (48)$$

$$R_{xx} = \frac{E_{0x}}{N_e e v_{0x}} = \frac{1}{N_e^2 e^2} \sum_{q_k} X_{q_k}^2 U(q_k)^2 \sum_{n=1}^{\infty} J_n^2(\cdot) \frac{\partial}{\partial \omega} \omega^2(q_k; \cdot) = \sum_{n=1}^{\infty} n! \frac{1}{N_e^2 e^2} \sum_{q_i} X_{q_i}^2 M(q_i)^2 \sum_{n=1}^{\infty} J_n^2(\cdot) \frac{\partial}{\partial \omega} \omega^2(q_i; \cdot) = \sum_{q_i} n!; \quad (49)$$



The parameters  $v_1$ ,  $v_2$  and  $T_e$  in these expressions should be determined by solving equations (27), (28) and (29) with zero  $v_0$ . The longitudinal photoresistivity is defined as

$$R_{xx} = R_{xx}^0 + R_{xx}^{(h)}; \quad (50)$$

with  $R_{xx}^0$  being the longitudinal magnetoresistivity in the absence of the radiation field.

Photoconductivity in semiconductors, in the absence or in the presence of magnetic fields, has long been known at low temperatures, and was understood to result from the effects of electron heating due to the absorption of the radiation field energy.<sup>5,25,26</sup> In our formulation, the photoconductivity arises not only from the hot-electron effect (electron temperature change), but also from the photon-assisted electron-impurity and electron-phonon scatterings. Although it is difficult to distinguish contributions to photoconductivity from different mechanisms when the applied terahertz field is strong, in the case of weak ac fields, the longitudinal photoresistivity can be written as the sum of two terms:

$$R_{xx} = R_{xx}^{(h)} + R_{xx}^{(op)}; \quad (51)$$

The first term  $R_{xx}^{(h)}$  is obtained through expanding Eq. (49) by the small parameter  $T_e = T_e - T$  and is the result of ac field induced electron temperature change, as that proposed first by Kogan for the case without a magnetic field.<sup>25</sup> After determining the small electron temperature change from energy-balance equation (29), we can write

$$R_{xx}^{(h)} = \left( \frac{\partial R_{xx}^0}{\partial T_e} \right) T_e; \quad (52)$$

Here

$$\left( \frac{\partial R_{xx}^0}{\partial T_e} \right)_{T_e=T} = \frac{\partial}{\partial T} R_{xx}^0 = \frac{2}{N_e^2 e^2} \sum_{q; k} q_k^2 M(q; k) \int_0^{\frac{q}{T}} n^0\left(\frac{q}{T}\right) \frac{\partial}{\partial q} J_2(q_k; q) dq; \quad (53)$$

and

$$T_e = \frac{2}{48} \sum_{q; k} \frac{q^2}{T^2} M(q; k) \int_0^{\frac{q}{T}} J_2(q_k; q) n^0\left(\frac{q}{T}\right) dq^3; \quad (54)$$

with

$$= \frac{1}{12} (v_1^2 + v_2^2) 4 N_e m^3 M_2(!; 0) \sum_{q; k} q_k^2 M(q; k) \int_0^{\frac{q}{T}} J_2(q_k; q) dq^3; \quad (55)$$

Note that the terms on the right hand side of Eq. (55) are respectively the changes of  $S_p$  and  $W$  induced by photon-assisted scatterings.

The second component of photoresistivity  $R_{xx}^{(op)}$  is the result of the photon-assisted scattering processes and ac field induced electron distribution change

$$R_{xx}^{(op)} = \frac{1}{4 N_e^2 e^2} (3v_{1x}^2 + 3v_{2x}^2 + v_{1y}^2 + v_{2y}^2) Q_2(!); \quad (56)$$

Where

$$Q_2(!) = \sum_{q_k} q_k^4 A_d(q_k; 0) - A_d(q_k; !) = !; \quad (57)$$

with

$$A_d(q_k; !) = U(q_k) \int_0^{\frac{q}{T}} \frac{\partial}{\partial q} J_2(q_k; q) dq + \sum_{q; k} M(q; k) \int_0^{\frac{q}{T}} \frac{\partial}{\partial q} J_2(q; k) dq; \quad (58)$$

In the weak ac field limit we can see from Eq. (39) that the amplitudes of time-dependent drift velocity are linearly dependent on the strength of applied THz fields. Consequently, the photoresistivity is proportional to the intensity of THz field. When the intensity of the driving field becomes strong, the dependence of photoconductivity on the strength of THz field exhibits a complicated behavior. At the same time, the contribution from the electron-temperature

change and nonthermal photon-assisted scattering are hybridized. At low lattice temperatures, the hot-electron effect is sufficiently strong and is generally the dominant mechanism for photoresistivity. At high temperature, however, when the polar optical phonon scattering provides an efficient energy dissipation channel, the photoconductivity is mainly contributed from nonthermal mechanism.

Recently, the photoconductivity CR at high temperature has been demonstrated in the experiment of Ref. 7. The remarkable peaks in photoconductivity are observed when the cyclotron frequency is closed to the frequency of terahertz elds. It is also found that, not only the height but also the width of CR peaks increases with increasing intensity of terahertz elds.

In order to illustrate CR in photoconductivity at high lattice temperatures, we have numerically evaluated the dc longitudinal photoresistivity of a magnetically-biased GaAs/AlGaAs heterojunction. The lattice temperature  $T$  is 150 K. The considered sample has electron density  $N_e = 2.0 \times 10^{15} \text{ m}^{-2}$  and 4.2 K linear mobility  $200 \text{ m}^2/\text{Vs}$ , similar to that used in the experiment of Ref. 7.

In Fig.4 the longitudinal photoresistivity induced by THz elds of frequency  $\omega = 4 \text{ THz}$  having several different amplitudes is plotted as a function of magnetic eld. The resonant structure near the cyclotron resonance position shows up clearly. Furthermore, with increasing strength of THz eld, the CR peaks ascend and the line shapes broaden. These features are in qualitative agreement with experimental results in Ref.7. In the inset of Fig.4 we plot the photoresistivity at CR as a function of the intensity of THz eld. One can see that the photoresistivity follows a linear dependence on the intensity of THz eld in the range  $0 < I_{\text{THz}} < 1 \text{ kW/cm}^2$ . For larger ac eld intensity, the deviation from linear dependence appears. The electron temperature also exhibits resonant peak when the cyclotron frequency is closed to the THz frequency, as shown in Fig.5. Nevertheless, since at high lattice temperatures the strong electron-LO phonon scattering provides an efficient energy dissipation channel, the rise of electron temperature is modest, and the hot-electron effect induced photoconductivity is small in comparison with the nonthermal effect. The photon-assisted scatterings are the main mechanisms for the photoconductivity at high temperature. For relative weak radiation eld, e.g.  $E_{\text{THz}} = 0.24 \text{ kV/cm}$ , the electron temperature has no appreciable difference from  $T$ , yet the  $R_{xx}$  still exhibits sizable resonance, comparable with the peak height observed in experiments of Ref. 7. In Fig.6 we plot the longitudinal photoresistivity as a function of magnetic eld strength for relatively weak ac elds. The contribution to photoconductivity from hot-electron effect is less than 3%. We also show the experimental observation<sup>7</sup> of CR in photoconductivity in the inset of Fig.6. The extraordinary width of the resonance shown in the experimental  $R_{xx}$  is possible due to the short pulse or large bandwidth of the terahertz radiation used in experiment, as explained in Ref. 7.

## VI. CONCLUSION

We have developed the momentum and energy balance equations for steady-state electron transport and optical absorption under the influence of a dc electric eld, an intense THz ac electric eld in a two-dimensional semiconductor in the presence of a strong magnetic eld perpendicular to the 2D plane. This formulation allows us to investigate the THz- eld-intensity dependence of the cyclotron resonance in transmittance and photoconductivity of GaAs/AlGaAs heterojunctions. We found that the CR peaks and line shapes of transmittance exhibit different behaviors when the intensity of the THz eld increases in the range above or below a certain critical value. The cyclotron resonance in photoresistivity, however, always enhances with increasing intensity of the THz eld. These results qualitatively agree with the experimental observations. The intensity-dependent behavior of transmittance at CR is explained as the result of combining hot-electron effect induced Landau level broadening and electron-phonon scattering enhancement, and the drift velocity dependence of the photon-assisted scattering matrix elements. We have also clarified that the CR in photoconductivity is not only the result of the electron heating, but also comes from photon-assisted scattering enhancement, especially at high temperatures. The effect of an intense THz eld on Faraday angle and ellipticity of magnetically-biased 2D semiconductor systems have also been demonstrated.

The authors gratefully acknowledge stimulating discussions with Drs. Bing Dong and W.S. Liu. This work was supported by the National Science Foundation of China (Grant Nos.60076011 and 90103027), the Special Funds for Major State Basic Research Project (Grant No.20000683), the Shanghai Municipal Commission of Science and Technology, and the Shanghai Postdoctoral Fellow Science Foundation.

---

Electronic address: liusy@mails.jtu.edu.cn

<sup>1</sup> J.Kono, A.H.Chin, A.P.Mitchell, T.Takahashi, and H.Akiyama, Appl.Phys.Lett. 75, 1119 (1999); G.A.Khodaparast, D.C.Larrabee, J.Kono, D.S.King, S.J.Chung, and M.B.Santos, Phys.Rev.B 67, 035307 (2003).

- <sup>2</sup> C. S. Ting, S. C. Ying, and J. J. Quinn, Phys. Rev. B 16, 5394 (1977).
- <sup>3</sup> G. A. Rodriguez, R. M. Hart, A. J. Sievers, F. Keilmann, Z. Schlesinger, S. L. Wright, and W. I. Wang, Appl. Phys. Lett. 49, 458 (1986).
- <sup>4</sup> J. C. Maan, Th. Englert, and D. C. Tsui, Appl. Phys. Lett. 40, 609 (1982).
- <sup>5</sup> K. Hirakawa, K. Yamataka, Y. Kawaguchi, M. Endo, M. Saeki, and S. Komiyama, Phys. Rev. B 63, 085320 (2001); Y. Kawaguchi, K. Hirakawa, M. Saeki, K. Yamataka, and S. Komiyama, Appl. Phys. Lett. 80, 136 (2002).
- <sup>6</sup> N. A. Morozovets and I. N. Kotel'nikov, Semiconductors 28, 1080 (1994).
- <sup>7</sup> P. M. Koentraad, R. A. Lewis, L. R. C. W. Aumans, C. J. G. M. Langerak, W. Xu, and J. H. Wolter, Physica B, 256-268, 268 (1998).
- <sup>8</sup> X. L. Lei, J. Appl. Phys. 84, 1396 (1998); J. Phys.: Condens. Matter 10, 3201 (1998).
- <sup>9</sup> X. L. Lei and S. Y. Liu, J. Phys.: Cond. Matter 12, 4655 (2000).
- <sup>10</sup> X. L. Lei and S. Y. Liu, Eur. Phys. J. B 13, 271 (2000).
- <sup>11</sup> X. L. Lei, J. L. Birman, and C. S. Ting, J. Appl. Phys. 58, 2270 (1985).
- <sup>12</sup> X. L. Lei and C. S. Ting, Phys. Rev. B 32, 1112 (1985).
- <sup>13</sup> A. Mayer and F. Keilmann, Phys. Rev. B 33, 6962 (1986).
- <sup>14</sup> X. L. Lei, J. Appl. Phys. 82, 718 (1997).
- <sup>15</sup> X. L. Lei and N. J. M. Horing, Int. J. Modem. Phys. B 6, 805 (1992).
- <sup>16</sup> D. R. Leadley, R. J. Nicholas, J. Singleton, W. Xu, F. M. Peeters, J. T. Devreese, J. A. J. Perenboom, L. van Bockstal, F. Herlach, J. J. Harris and C. T. Foxon, Phys. Rev. B 48, 5457 (1993); Phys. Rev. Lett. 73, 589 (1994).
- <sup>17</sup> R. R. Gerhardt, Z. Phys. B 21, 275 (1975).
- <sup>18</sup> T. Ando, J. Phys. Soc. Jpn. 38, 989 (1975).
- <sup>19</sup> See, e.g. V. Gudmundsson and R. R. Gerhardt, Phys. Rev. B 35, 8005 (1987), and references therein.
- <sup>20</sup> D. J. Barnes, R. J. Nicholas, F. M. Peeters, X.-G. Wu, J. T. Devreese, J. Singleton, C. J. G. M. Langerak, J. J. Harris, and C. T. Foxon, Phys. Rev. Lett. 66, 794 (1991).
- <sup>21</sup> K. W. Chiu, T. K. Lee, and J. J. Quinn, Surf. Sci. 58, 182 (1976).
- <sup>22</sup> For recent theoretical work, see, e.g., V. V. Popov and T. V. Teperik, JETP Lett. 70, 254 (1999).
- <sup>23</sup> R. F. O'Connell and G. Wallace, Phys. Rev. B 26, 2231 (1982).
- <sup>24</sup> V. A. Volkov, D. V. Galchenkov, L. A. Galchenkov, I. M. G. rodnenskii, O. R. Matov, S. A. Mikhailov, A. P. Senichkin, and K. V. Starostin, JETP Lett. 43, 326 (1986).
- <sup>25</sup> Sh. M. Kogan, Sov. Phys. Solid State 4, 1386 (1963).
- <sup>26</sup> P. M. Valov, B. S. Ryvkin, I. D. Yaroshetskii, and I. N. Yassievich, Sov. Phys. Semicond. 5, 797 (1971).

### Figure Captions

FIG. 1. The intensity-dependence of 2D semiconductor transmittance and electron temperature, is plotted at cyclotron resonance position,  $\omega_c = \omega$ . The transmittance is normalized to the value of zero magnetic field. The THz fields with two different frequency  $\omega = 0.83$  and  $\omega = 1.6$  THz are exposed to the studied 2D system. The lattice temperature is  $T = 42$  K. Experimental results of transmittance versus the intensity of THz fields  $I_{is}$  (Fig. 2 of Ref. 3) is reproduced in the inset.

FIG. 2. The cyclotron resonance of 2D semiconductor transmittance of several incident electromagnetic fields with a same frequency  $\omega = 0.83$  THz but different intensity  $I_{is} = 0.1, 0.6, 74, 750, 1500, 2500$  W/cm<sup>2</sup>.

FIG. 3. The Faraday angle  $\theta_F$  and ellipticity  $\eta$  are plotted as functions of the strength of magnetic fields  $B$  for the same system and under the same condition as described in Fig. 2.

FIG. 4. The cyclotron resonance in the longitudinal resistivity change  $R_{xx}$  induced by a radiation field of frequency  $\omega = 4$  THz having several different amplitudes  $E_{is} = 0.24, 0.61, 0.87, 1.1, 1.2$  kV/cm. The lattice temperature is  $T = 150$  K. The inset shows  $R_{xx}$  versus intensity of incident THz fields  $I_{is}$  at  $\omega_c = \omega$ .

FIG. 5. The cyclotron resonance in electron temperature  $T_e$  for the same system and under the same condition as described in Fig. 4.

FIG. 6. Similar to the Fig. 4, but the strength of THz fields are relatively weak  $E_{is} = 0.086, 0.13, 0.19, 0.24$  kV/cm. The experimental results (Fig. 3 of Ref. 7) of the cyclotron resonance in photoconductivity is shown in the inset.

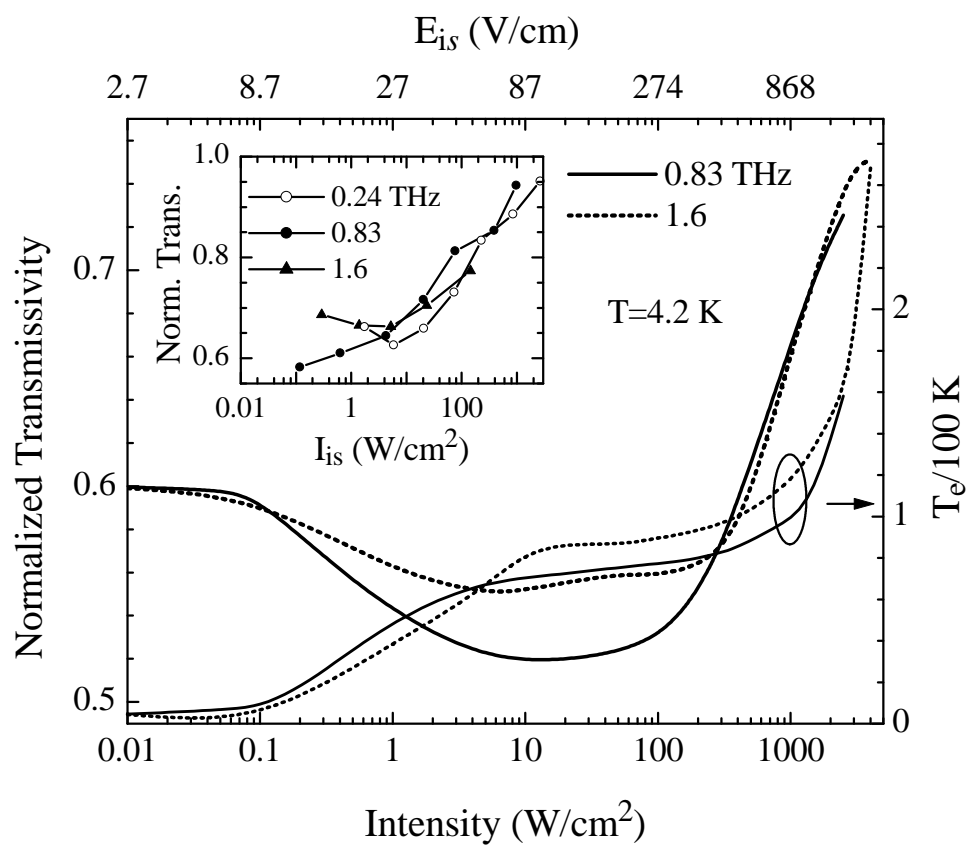


Fig. 1

Liu & Lei

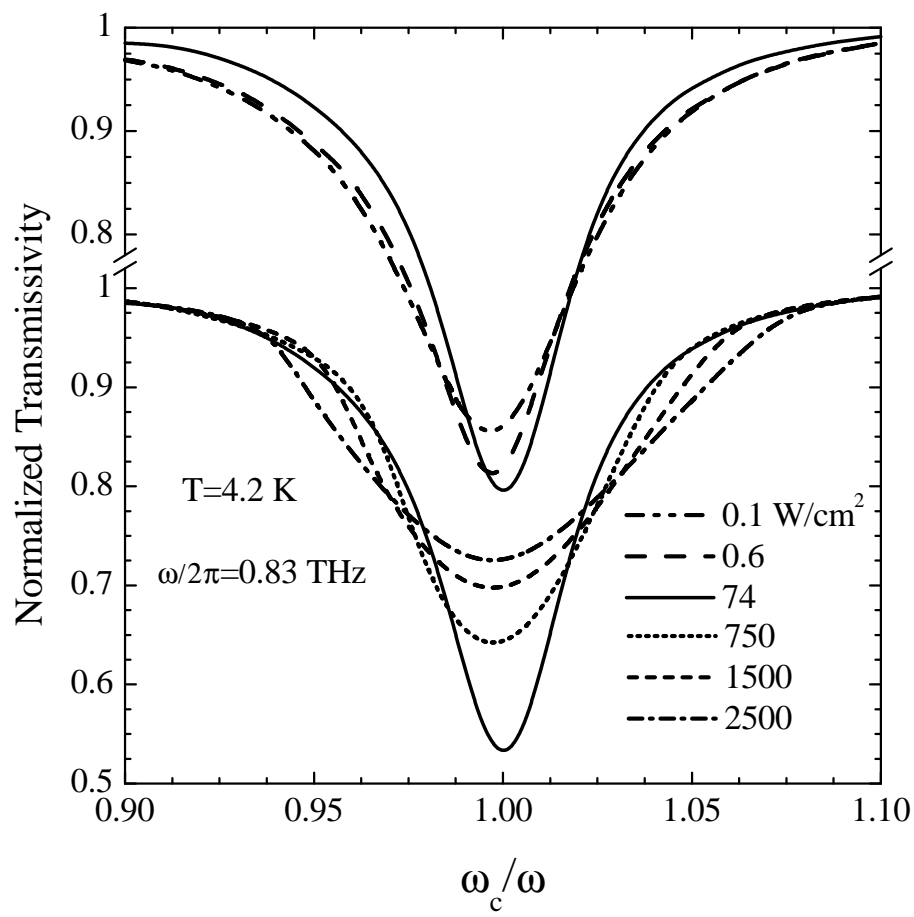


Fig. 2

Liu & Lei



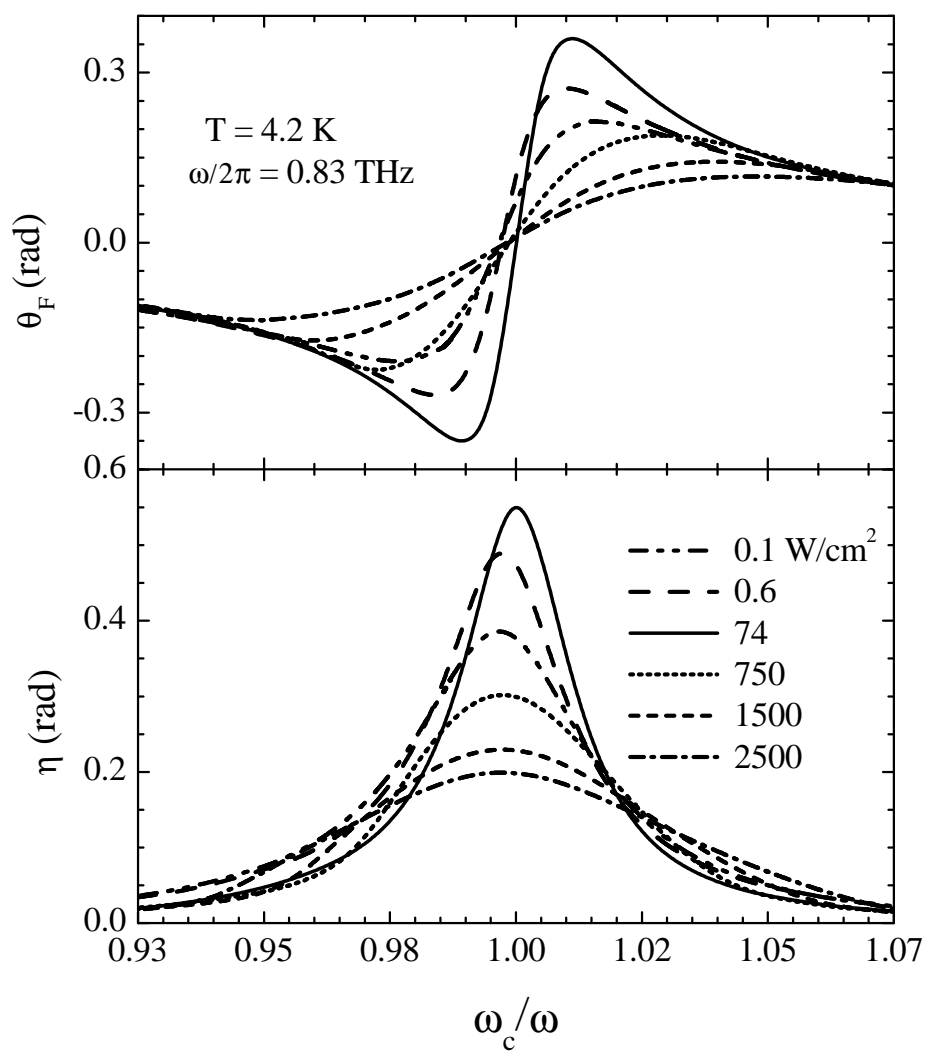


Fig. 3

Liu & Lei





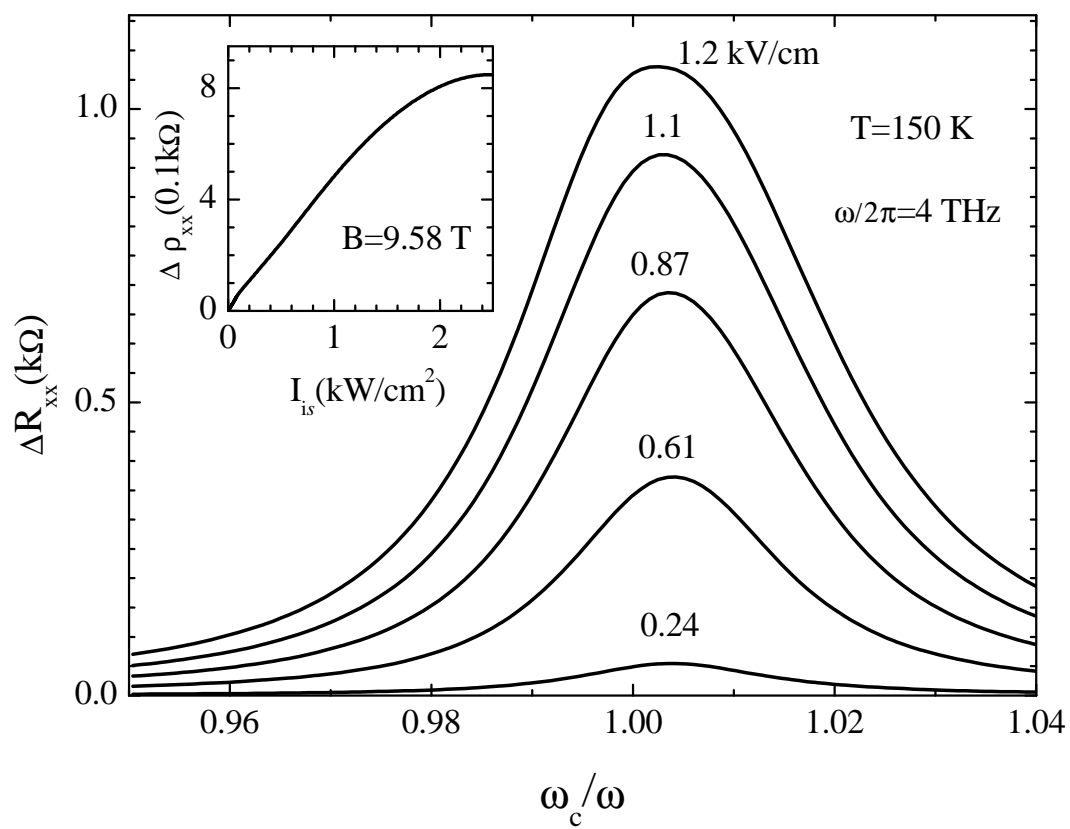


Fig. 4

Liu & Lei



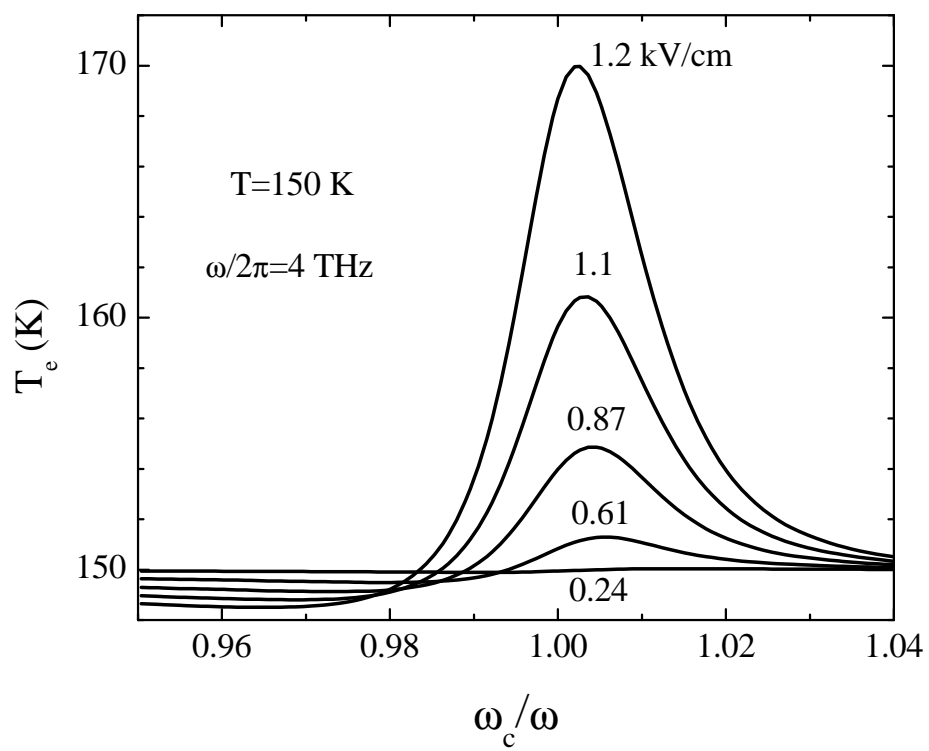


Fig. 5

Liu & Lei



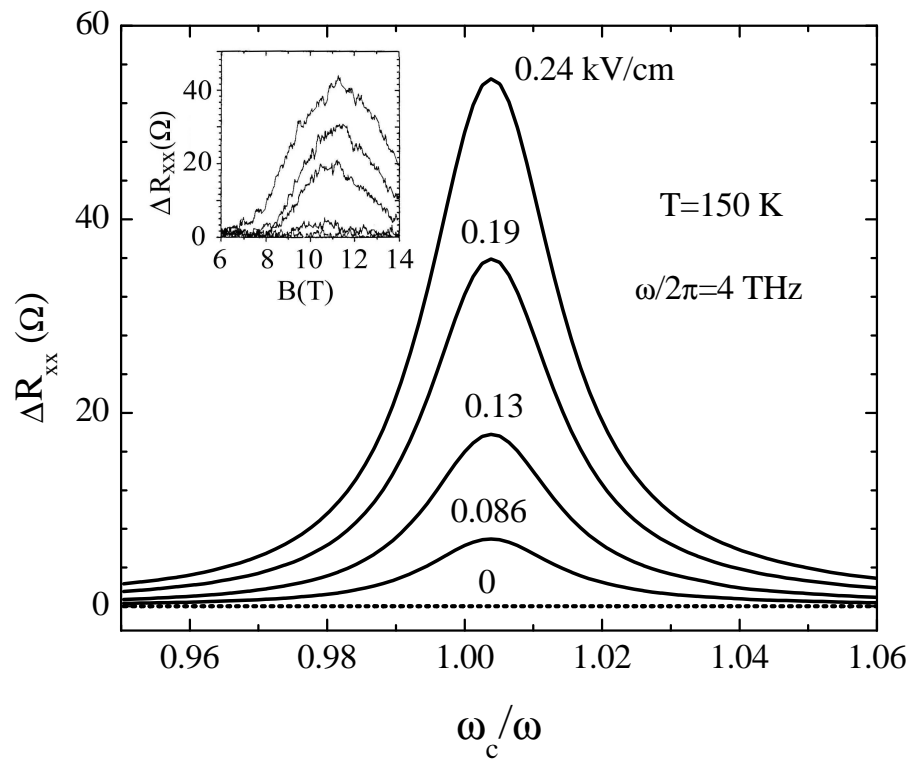


Fig. 6

Liu & Lei